International Journal of Chemical, Materials and Biomolecular Sciences
ISSN: 2415-6620
Vol:4, No:1, 2010

Finite Element Modeling of Rotating Mixing of Toothpaste

Inamullah Bhatti[a*], Ahsanullah Baloch[b] and Khadija Qureshi[a]

***Abstract*—**The objective of this research is to examine the shear thinning behaviour of mixing flow of non-Newtonian fluid like toothpaste in the dissolution container with rotating stirrer. The problem under investigation is related to the chemical industry. Mixing of fluid is performed in a cylindrical container with rotating stirrer, where stirrer is eccentrically placed on the lid of the container. For the simulation purpose the associated motion of the fluid is considered as revolving of the container, with stick stirrer. For numerical prediction, a time-stepping finite element algorithm in a cylindrical polar coordinate system is adopted based on semi-implicit Taylor-Galerkin/pressure-correction scheme. Numerical solutions are obtained for non-Newtonian fluids employing power law model. Variations with power law index have been analysed, with respect to the flow structure and pressure drop.

***Keywords*—**finite element simulation; mixing fluid; rheology; rotating flow; toothpaste

I. INTRODUCTION

THE design of the mixer with rotational mixing in a stirred container to predict shear stress and power consumption is of industrial importance. Industrial problems are complex to resolve, mainly associated with the nature of chemical process industry, for instance mixing and in paper industry combining of paper pulp, mixing of powders, granular mixing processes [1–10]. In numerous mixing and blending processes the use of stirrer, the difficult features are with different shapes and locations may be with or without agitators, the rotating speed and the use of the complex fluids. In the process of tooth–paste preparation the viscosity increases due to the addition of solid ingredients or due to its change in the size and leads to increase in shear stress rate. Shear stress in non Newtonian fluid causes to increase strain in the circular tank, due to which more power is consumed to homogenise it [11–12]. Therefore, the strength of the agitator shaft and the walls of the tank may not sustain to the shear force [13]. Present investigation study this behaviour through predicting the shear-rate, pressure differential, flow structure, shear-stress, shear velocity gradient and work done.

In this study, the non-Newtonian behaviour of the Tooth paste is focused in the circular tank with asymmetric stirrer(s) located at eccentric position by using the Power Law Model [11–12]. In Computational Fluid Dynamics (CFD), complex flows of non-Newtonian fluids are modelled through non–linear system of partial differential equations, such as generalised momentum equations in cylindrical polar coordinate system to determine the pressure and velocities of fluid and the stress of real fluids.

Finite Element Method (FEM) is a powerful tool for the analysis of heat and mass transfer problems of common interest, and it is used to accurately model the domain boundaries, which is the major advantage of the (FEM) [14]. The quality of predictions are based on different features comprise mostly the division of spatial discretisation for whole domain, time discretisation for transient problem, selection of suitable material properties and appropriate treatment of boundary conditions [15]. All these characteristic of setting up a problem require thoroughness and experience, and are considered in the prediction of numerical solutions.

For the simulation of incompressible fluids the present study adopts a time–marching algorithm namely, semi-implicit Taylor–Galerkin/pressure–correction scheme [14–18]. The problem specification is defined in Section 2, for the simulations, Section 3 presents the details on the governing system of equations and numerical method employed. Simulated solution is presented in Section 4 and Section 5 describes the conclusions.

II. PROBLEM SPECIFICATION

Two-dimensional mixing flow of non-Newtonian fluids is investigated relevance to the pharmaceutical/ cosmetic industry. To predict rheological behaviour of toothpaste, within industrial process, the stirrer is eccentrically fixed with the lid of the container [16–18]. However, here, for simulations, the mixing is performed through the rotation of cylindrical–type container and the stirrer is fixed on to the lid of the container remain stationary. Firstly, the problem is considered for the mixing of Newtonian material with stationary stirrer in rotating cylindrical container, to compare the predictions with the solutions achieved by the other researchers [16–18].

Inamullah Bhatti is assistant professor in the department of chemical engineering of Mehran University of Engineering & Technology Jamshoro he graduated in 1995 from the same department and joined as lecturer in 1996. He has more the 12 research publications and conferences proceedings. Mr. Bhatti did his masters of engineering from MUET in 2008 on the non Newtonian behaviour of toothpaste and this work is produced from his masters project.bhatti_inam@yahoo.com

Dr. Ahsanullah Baloch is professor in the department of BS&RS MUET, Jamshoro. He did his doctorate and post doctorate from Swansea University UK. He has more than 50 research publication. His contribution in the field of computation is remarkable.

Dr. Khadija Qureshi is first Pakistani women having doctorate in the chemical engineering. She has more than 20 research papers presented in the international conferences and published in ISI Journals.qureshi.khadija@yahoo.com

Three–dimensional domain (a) along with two–dimensional slice (b) and finite element mesh (c) for the problem concerned is presented in Figure–1.

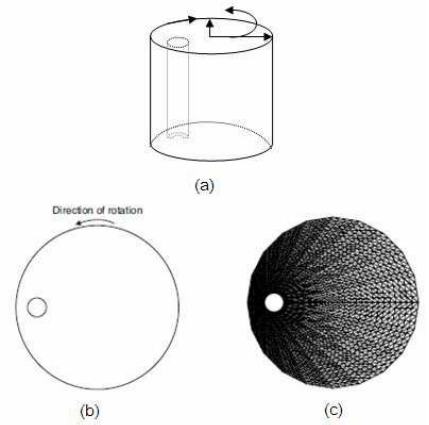

Fig. 1 Eccentric rotating flow, with single fixed stirrer; (a) three dimensional domain; (b) two dimensional slice (c) finite element mesh.

The present study investigates the two-dimensional mixing flows of non-Newtonian fluid, relevance to the chemical industry for instance occurs in toothpaste mixing. Ideally, the motion of the fluid is determined by the circular motion of the stirrer remains fixed with lid of the container and for simulations. A fixed stirrer in an eccentric configuration is adopted. The problem for circular flow between stationary stirrer and rotating cylindrical container has been examined. To confirm the numerical solutions, cylindrical co-ordinates are employed to contrast against other numerical results [16–18]. For mesh convergence three different meshes were used in the simulations, however, here predicted results are presented only on intermediate mesh M2. For mesh M2, the total number of elements is 3840; the total number of nodes 7840 and the degrees-of-freedom are 17680.

For the well prediction of the flow problem, it is essential to impose suitable initial and boundary conditions. Simulation starts from a zero initial condition. For motionless stirrer, the velocity components vanishes on the solid surface of stirrer ($v_r = 0$ and $v_\theta = 0$) [9]. On the rotating cylinder container wall a fixed velocity boundary condition is applied ($v_r = 0$ and $v_\theta = 1$), and a vanishing pressure condition is specified [16–18]. Vanishing stream function is fixed on cylinder and Neauman boundary condition is applied on the stirrer.

III. System of Equations and Numerical Algorithm

Consider the two-dimensional isothermal flow for Newtonian fluid in cylindrical coordinate system, a system consisting of the mass conservation and generalized unsteady momentum equations over domain Ω. The system of equations, without body forces, can be denoted by the continuity equation, as,

$$\nabla \cdot u = 0, \quad (1)$$

and the momentum transport equation, as,

$$\rho \frac{\partial \boldsymbol{u}}{\partial t} = \nabla . \quad - \rho \boldsymbol{u} . \nabla \boldsymbol{u} \quad , \quad (2)$$

where, ρ is the fluid density (per unit mass), u is the fluid velocity, t represents time, σ is the Cauchy stress tensor can be expressed as σ = −pδ + T, and ∇ the spatial differential operator. Whilst p is the isotropic fluid pressure (per unit density), δ is the Kronecker delta tensor, whilst T is a total stress tensor. For Newtonian fluid the stress tensor T is given as:

$$T = 2\mu d, \quad (3)$$

where d is the rate-of-deformation tensor given as $\mathbf{d} = \frac{1}{2}[\nabla u + (\nabla u)^t]$ and μ is the associated fluid viscosity, constant for Newtonian case. Non-dimensional Reynolds number is defined as: $Re = \frac{\rho V_c R}{\mu_c}$. R is the characteristic radius of the stirrer as a length scale, the rotating speed of the container equal to 50 rpm taken as characteristic velocity V_c, and μ_c viscosity is the characteristic zero shear-rate viscosity of 105 Pa s. Appropriate scaling in each variable yields dimensional variables $p = 2444\ p^*$.

Toothpaste is considered as Pseudo plastic fluid in the terms of rheological behaviour. It contains suspensions and pharmaceutical material which develops the form of the flow curve is determined by power law equation [11]. For a generalised inelastic non-Newtonian fluid, stress tensor T can be expressed as $T = 2\mu(\dot{\gamma})d$, where $\mu(\dot{\gamma})$ is the shear-rate ($\dot{\gamma}$) dependent functional viscosity. For the Power Law model, the viscosity structure: $\mu(\dot{\gamma}) = k\ \dot{\gamma}^{m-1}$, where k is the apparent zero shear-rate viscosity obtained from the Newtonian fluids (see Figure–2), and m is index for power-law. In figure–2, Pa s refer to the units of viscosity with reciprocal seconds on shear-rate. Then the power law equation decreases in viscosity with increasing the shear-rate as follows:

Shear-rate $\dot{\gamma} = 2\sqrt{|I_2|}$, second invariant of rate of strain tensor is I_2, which is elaborated in details as under:

$$I_2 = \frac{1}{2} trace(\mathrm{d}^2), I_2 = \frac{1}{\mathrm{r}} trace\ (\mathrm{D}^2),$$

$$d = \begin{bmatrix} 2\frac{\partial v_r}{\partial r} & \frac{\partial v_\theta}{\partial r} + \frac{1}{r}\frac{\partial v_r}{\partial \theta} \\ \frac{\partial v_\theta}{\partial r} + \frac{1}{r}\frac{\partial v_r}{\partial \theta} & \frac{2}{r}\frac{\partial v_\theta}{\partial \theta} + 2\frac{v_r}{r} \end{bmatrix}$$

To compute numerical solutions a time-stepping finite element algorithm is adopted in present study through a semi-implicit Taylor-Galerkin/pressure-correction scheme [16–18], established on a fractional-stege formulation. This comprises of discretisation, first in the temporal domain through Taylor series expansion in time and to build a second-order time-stepping scheme a pressure-correction method is adopted. For spatial discretisation, Galerkin approximation is employed momentum equation.

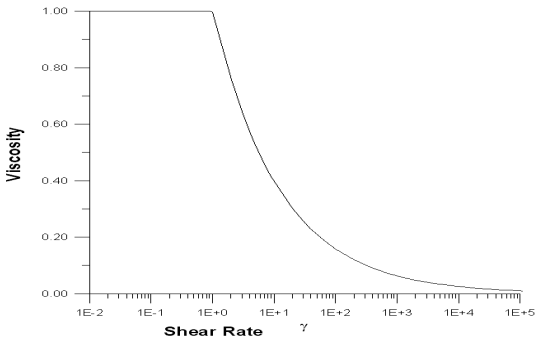

Fig. 2 Viscosity behaviour of toothpaste using Power law model

The linear (ψ_k) and quadratic (φ_j) basis functions are used for pressure and velocities respectively. To estimate subsequent integrals a seven point Gauss quadrature rule.

Stage 1a:

$$\left[\frac{2\boldsymbol{M}}{\Delta t}+\frac{\boldsymbol{S}}{2\,\mathrm{Re}}\right]\left(V_r^{n+\frac{1}{2}}-V_r^{n}\right)=\frac{-\mu_c}{\mathrm{Re}}\left\{S_{rr}V_r+S_{r\theta}V_\theta\right\}^n-\left\{\boldsymbol{N}(\boldsymbol{V})V_r-N_1(V_\theta)V_\theta\right\}^n+L_r^{\dagger}P^n$$

$$\left[\frac{2\boldsymbol{M}}{\Delta t}+\frac{\boldsymbol{S}}{2\,\mathrm{Re}}\right]\left(V_\theta^{n+\frac{1}{2}}-V_\theta^{n}\right)=\frac{-\mu_c}{\mathrm{Re}}\left\{S_{r\theta}^{\dagger}V_r+S_{\theta\theta}V_\theta\right\}^n-\left\{\boldsymbol{N}(\boldsymbol{V})V_\theta-N_1(V_\theta)V_r\right\}^n+L_\theta^{\dagger}P^n$$

Stage 1b:

$$\left[\frac{2\boldsymbol{M}}{\Delta t}+\frac{\boldsymbol{S}}{2\,\mathrm{Re}}\right]\left(V_r^{*}-V_r^{n}\right)=\frac{-\mu_c}{\mathrm{Re}}\left\{S_{rr}V_r+S_{r\theta}V_\theta\right\}^n-\left\{\boldsymbol{N}(\boldsymbol{V})V_r-N_1(V_\theta)V_\theta\right\}^{n+\frac{1}{2}}+L_r^{\dagger}P^n$$

$$\left[\frac{2\boldsymbol{M}}{\Delta t}+\frac{\boldsymbol{S}}{2\,\mathrm{Re}}\right]\left(V_\theta^{*}-V_\theta^{n}\right)=\frac{-\mu_c}{\mathrm{Re}}\left\{S_{r\theta}^{\dagger}V_r+S_{\theta\theta}V_\theta\right\}^n-\left\{\boldsymbol{N}(\boldsymbol{V})V_\theta-N_1(V_\theta)V_r\right\}^{n+\frac{1}{2}}+L_\theta^{\dagger}P^n$$

Stage 2:

$$\theta\mathbf{K}\,\mathrm{Q}^{n+1}=\frac{1}{\Delta t}\mathbf{L}\mathbf{V}^{*}$$

Stage 3:

$$\frac{M}{\Delta t}\left(\mathbf{V}^{\mathrm{n}+1}-\mathbf{V}^{*}\right)=-\theta\mathbf{L}\mathrm{Q}^{n+1}$$

,

where V^n , V^* and V^{n+1} are the nodal velocity vectors at time t_n, an intermediate non-solenoidal velocity vector and a solenoidal velocity vector at time step t^{n+1}, respectively. P^n and $Q^{n+1} = P^{n+1} - P^n$ are pressure and a pressure difference vectors respectively. Where as M, N(V), K, L and S are the mass, the convection, the pressure stiffness, the divergence/pressure gradient and the momentum diffusion matrices respectively. The definition of the above system matrices and details on numerical scheme are given in ref. [8]. Here, time step index is denoted by n.

To provide the particular second-order form of the pressure-correction algorithm the Crank–Nicolson coefficient θ is considered as 1/2. In addition, at stage–1, for diffusion terms an implicit treatment is employed through a Crank-Nicolson distribution to the LHS of the momentum equation.

The components of velocity at the n + $\frac{1}{2}$ time step are computed at step 1a and at step 1b an intermediate velocity V^* is computed. At the full time step n + 1 velocity components are computed by means of the solutions at the level n and n + $\frac{1}{2}$. Jacobi iterative technique that requires only a few numbers of iterations is used at first and third stages for mass matrices. At step two, Poisson equation appears, is computed for the pressure-difference from a non-divergence free velocity. Due to symmetric, bended and positive-definite nature of stiffness matrix for Poisson equation it is suitable to adopt a direct Choleski method. A divergence free velocity is calculated from the pressure-difference of second stage at the closing stage of the time-step cycle for third and final step.

The generalized weighting function w_i replaces φ_i, for the Galerkin formulation of momentum equation in finite element approximation. In general, the time-step (Δt) equal to 10^{-2}, and tolerance of 10^{-5}, the relative solution-increment for time-step termination is enforced [18–21].

Herein numerical results are presented via pressure isobars, contours of stream function and Newtonian stress components. Also solution of interest, shear-rate ($\dot{\gamma}=\sqrt{2I_2}$), local rate-of-work done ($\dot{\omega}=T:\nabla v$,T is the total stress tensor, ∇ is spatial differential operator and v is the fluid velocity in given domain Ω), power ($\dot{P}=\int_{\Omega}\dot{\omega}(x,t)d\Omega$) and total work done ($W=\int_{T}P(t)dt$) are presented.

IV. Numerical Results

A. Field Data

For Colgate toothpaste the field data was obtained from the Colgate and Palmolive Industries, Kotri. The specific gravity of the tooth paste is 1.5, viscosity is 170000 centipoises, volume of the container 900 Kg and the rotational speed of the homogenizer is 1400 rpm. The characteristic values are applied to calculate the non–dimensional Reynolds number which is about 20 and the numerical results are also computed for higher and lower Reynolds numbers to compare the influence of inertia.

The predictions are considered from two different situations: with increasing the Reynolds number for Newtonian flow behaviour (Re = 10, 20 and 30) and decreasing the Power law number for Non-Newtonian behaviour of the toothpaste (n = 0.9, 0.8, 0.7 and 0.6). The predictions are illustrated by means of contour of streamlines, pressure isobars, shear gradients, shear stresses and shear rates for Newtonian and non-Newtonian behaviour of toothpaste. From the real data of the toothpaste viscosity and density applied in the industry, calculated in the lab is used to develop the Reynolds number (Re = 30) and for toothpaste Power law number (n = 0.6) is considered for Non-Newtonian behaviour [12].

B. Flow structures and pressure differential for Newtonian behavior

The impact of increasing Reynolds number upon flow structures and pressure differential are illustrated in figure 3 in contour plots for Newtonian flow behavior. Computations are

carried out at Re = 10, 20 and 30. At small values of inertia, i.e. Re = 10, a strong vortex forms in the core of the cylindrical container. Flow structure remains unaffected though upon enhancing the Reynolds number up to Re = 30 inertia takes control and the vortex turn and moves towards the upper half of the container, eddy intensity diminish and the eddy centre is pressed near the container wall. The decreasing trend in re-circulating flow rate is tabulated in Table 1.

TABLE I
EDDY INTENSITY AND PRESSURE DROP FOR NEWTONIAN BEHAVIOUR

Reynolds Numbers	Eddy Intensity		Pressure Isobars	
	Min	Max	Min	Max
10	0	4.782	-5.704	3.593
20	0	4.455	-8.571	3.679
30	0	4.206	-11.672	3.609

For pressure differential, similar symmetry arguments apply at Re = 10 and pressure isobars emerge in symmetric fashion by equivalent degree in both negative and positive intensity on the upper side and lower side of the stirrer in constricted place. As inertia augmented from Re = 10 to Re = 30, asymmetric patterns are experienced, with minima at the lower side of the stirrer and maxima on the upper side of the stirrer.

C. Pressure differential and flow structures for non-Newtonian behaviour

The effect of decreasing the power law number (n=0.9 to n=0.6) upon streamline patterns are displayed in Fig. 4 and pressure differential in Fig. 5 are represented in contour plots for Non-Newtonian fluid. In fact the flow structure or the change in position of recirculation irrespective of the magnitude of inertia is not affected by shear thinning behaviour. While, decreasing the power law number more twist is observed in asymmetric eddy in the way of the container motion [13]. Shear thinning property is observed to advance the transfer of vortex centre towards the wall of the container l and diminish the re-circulating flow rate. Largely, shear thinning effects have only a slight influence on the streamlines. The contour result of pressure difference is very much identical; as the power law number decreases it is shifting from the wall sides to the centre of container [14]. Whereas the negative maximum values are on the lower side of stirrer tip which effects the stretching and the maximum is at the centre of container. The values are tabulated in Table 2.

D. Work study for Newtonian and non-Newtonian behaviour of toothpaste

Computations are performed with respect to time for Newtonian and non-Newtonian behaviour at Reynolds number Re = 20 and decreasing the power law number from n = 0.9 to n = 0.6 for non-Newtonian. Power as sum of work done, rate of work done and total work done is shown using line plots in fig. 6 and 7. For Newtonian behaviour at Reynolds

TABLE II
EDDY INTENSITY AND PRESSURE DROP FOR NON-NEWTONIAN BEHAVIOUR AT RE = 20

Power Law Index	Eddy Intensity		Pressure Isobars	
	Min	Max	Min	Max
0.9	0	4.532	-8.908	3.848
0.8	0	4.636	-9.081	4.279
0.7	0	4.785	-10.963	10.976
0.6	0	4.934	-11.154	16.016

number 20, the work is higher than unity, rate of work done and total work done become flatten at about 3000 time steps at $\Delta t = 10^{-3}$. Whereas for non-Newtonian behaviour with decreasing the power law numbers the predictions are totally different and the results are indicating the rapid changes for the rate of work done and total work done, as shown in the line plots, fig. 7. As time marches, some instability is observed for low power law index and after considerable time solution shows stable behaviour, see fig. 7.

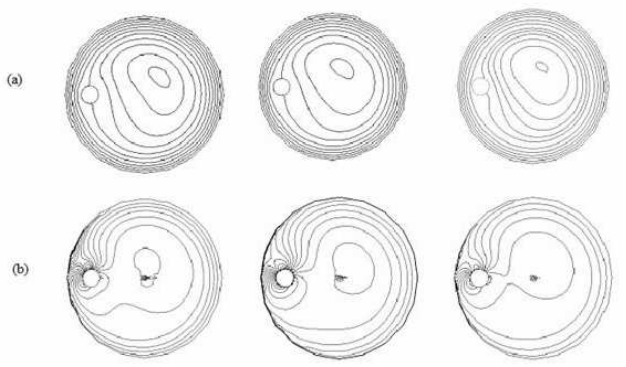

Fig. 3 For Newtonian flow behaviour with increasing Reynolds number (a) Streamline contours and (b) pressure isobars.

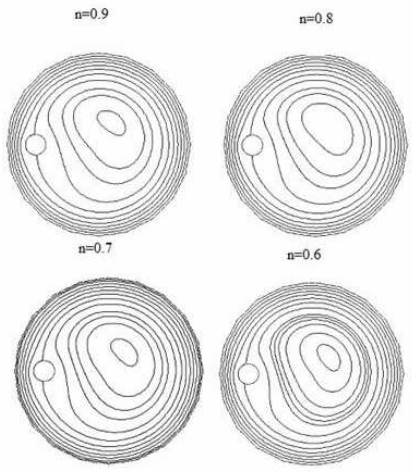

Fig. 4. Streamline Contours of non-Newtonian behaviour of toothpaste at reducing power law numbers.

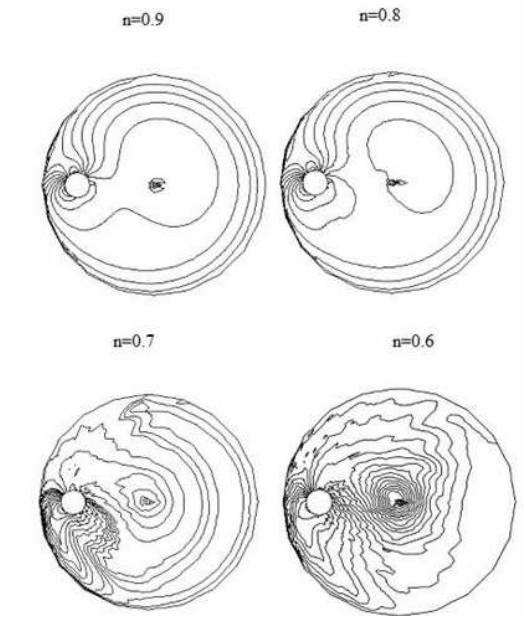

Fig. 5. Pressure Isobars of Non Newtonian Behaviour of toothpaste at decreasing power law numbers

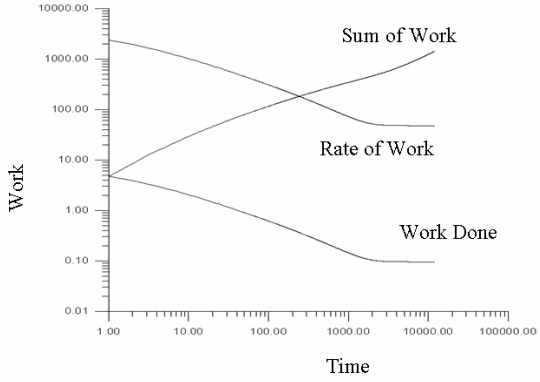

Fig. 6. Work calculation with respect to time for Newtonian behaviour at Re = 20

V. Conclusions

Finite element algorithm employed to develop a computational model for rotational flow of non-Newtonian fluid like toothpaste in the circular tank successfully applied to predict the shear rate in the mixing. It is clearly demonstrated that with increasing the inertia fluid flow structure in mixing tank loses its equilibrium and vortex shift upward in the direction of container movement and non-dimensional pressure differential enhances. The pressure differential are generally higher in the non-Newtonian power law fluid when the power law number is decreased to the n= 0.6.

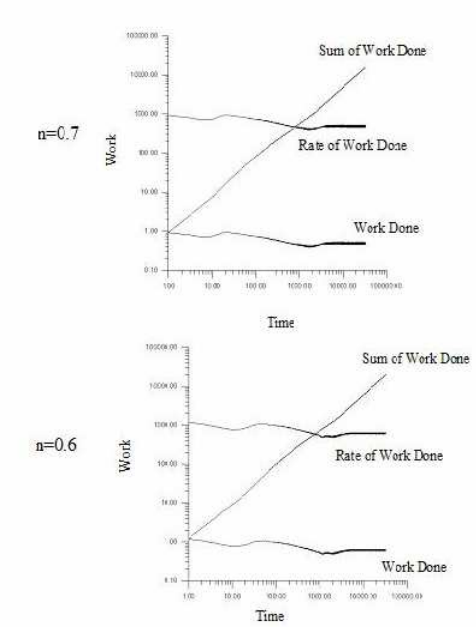

Fig. 7. Comparing the work calculation with respect to time for Non-Newtonian Behaviour of toothpaste at Re = 20, for Power law index number (n = 0.7 and n = 0.6).

The total work-done with respect to the time predicted by the model is indicating sum of work done and work done in the non-Newtonian behaviour is very much unstable and the fluctuation in this is very high as compared to the Newtonian behaviour. It is observed that the less work is required at the power law number n=0.7 for non-Newtonian behaviour of toothpaste, which is presented in the figure–7. The optimal rate of work with respect to time is predicted by the model and plotted on the graph is less than unity at power law number n = 0.7, when we compare this power law number to the others graphically plotted and shown in figure 7 and 8 is very much visible. The effect of shear thinning is predicted by the shear rate which is maximum 21.424 at power law index n = 0.7. From the numerical results generated, the design of mixer that will ultimately impact upon the mixing of tooth paste is related.

Acknowledgements

The authors greatly acknowledge the help and support of Chemical Engineering department, Mehran University of Engineering and Technology, Jamshoro, for providing computational facility. The work has been carried on the basis of theoretical data provided by the Colgate and Palmolive Industries.

References

[1] Portillo, P. M., Muzzio, F. J. and Ierapetritou, M. G., 'Hybrid DEM-Compartment Modelling Approach for Granular Mixing', AIChE Journal, 53(1), 119–128, 2007.
[2] Zlokarnik, M., "Stirring: Theory and Practice", Wiley-VCH, Weinheim, 2001.

[3] Wichterle, K. and Wein, O., "Threshold of mixing of non-Newtonian liquids", Int. Chem. Eng. V. 21, pp. 116–121, 1981.
[4] Luo, J. Y., Gosman, A. D., and Issa, R. I., "Prediction of impeller induced flows in mixing containers using multiple frames of reference", Inst. Chem. Eng. Symp. Ser., V. 136, pp. 549–556, 1994.
[5] Deen, N. G., Solberg, T., and Hjertager, B. H., "Flow generated by an aerated Rushton impeller: two-phase PIV experiments and numerical simulations", Can. J. Chem. Eng. V. 80, pp. 1–15, 2002.
[6] Tabor, G., Gosman, A. D., and Issa, R., "Numerical simulation of the flow in a mixing container stirred by a Rushton turbine", Inst. Chem. Eng. Symp. Ser. V. 140, pp. 25–34, 1996.
[7] Jaworski, Z. and Nienow, A. W., "LDA measurements of flow fields with Hydrofoil impellers in fluids with different rheological properties", Proceedings of 8th European Conference on Mixing, Cambridge, UK, pp. 105–112, 1993.
[8] Lane, G. and Koh, P. T. L., "CFD simulation of a Rushton turbine in a baffled tank", Proceedings of International Conference on Computational Fluid Dynamics in Mineral and Metal Processing and Power Generation, CSIRO, Melbourne, pp. 377–385, 1997.
[9] Buwa, V., Dewan, A., Nasser, A. F. and Durst, F., "Fluid dynamics and mixing of single-phase flow in a stirred container with a grid disc impeller: experimental and numerical investigations", Chem. Eng. Sci. V. 61, pp. 2815–2822, 2006.
[10] Saeed, S., Ein-Mozaffari, F. and Upreti, S. R., "Using computational fluid dynamics modelling and ultrasonic Doppler velocimetry to study pulp suspension mixing", Ind. Eng. Chem. Res. V. 46, pp. 2172–2179, 2007.
[11] Murthy, S. S. and Jayanti, S., "Mixing of power-law fluids using anchors: Metzner-Otto concept revisited", AIChE J. V.49, pp. 30–40, 2003.
[12] Kelly, W. and Gigas, B., "Using CFD to predict the behaviour of power law fluids near axial-flow impellers operating in the transitional flow regime", Chem. Eng. Sci. V. 58, pp. 2141–2152, 2003.
[13] Moore, I. P. T., Cossor, G. and Baker, M. R., "Velocity distributions in a stirred tank containing a yield stress fluid", Chem. Eng. Sci., V. 50, pp. 2467–2481, 1995.
[14] Townsend, P. and Webster, M. F., 'An algorithm for the three-dimensional transient simulation of non-Newtonian fluid flows', in: G. Pande, J. Middleton (Eds.), Proc. Int. Conf. Num. Meth. Eng.: Theory and Applications, NUMETA, Nijhoff, Dordrecht, pp. T12/1–11, 1987.
[15] Hawken, D. M., Tamaddon-Jahromi, H. R., Townsend, P., Webster, M. F., 'A Taylor-Galerkin-based algorithm for viscous incompressible flow', Int. J. Num. Meth. Fluids, 10, 327–351, 1990.
[16] Baloch, A., Grant, P. W. and Webster, M. F., "Parallel computation of two dimensional rotational flows of viscoelastic fluids in cylindrical container", Int. Journal for computer-Aided Engineering and Software, V. 19, No. 7, pp. 820-853, 2002.
[17] Baloch, A., Solangi, M. A. and Memon, G. Q., 'Simulation of Rotational Flows in Cylindrical Container with Rotating Single Stirrer', Punjab University Journal of Mathematics, 2008.
[18] Baloch, A., and Webster, M. F., 'Distributed Parallel Computation for Complex Rotating Flows of Non-Newtonian Fluids', Int. J. Numer. Meth. Fluids, 43, 1301-1328, 2003.